Vol 18 No 11, November 2009
1674-1056/2009/18(11)/4924-08

Chinese Physics B

© 2009 Chin. Phys. Soc.
and IOP Publishing Ltd

Bloch oscillation and Landau–Zener tunnelling in a modulated optical lattice in a photovoltaic photorefractive crystal*

Zhang Bing-Zhi(张冰志), Cui Hu(崔 虎),
Li Xiang-Heng(李湘衡), and She Wei-Long(佘卫龙)†
State Key Laboratory of Optoelectronic Materials and Technologies, Sun Yat-Sen University, Guangzhou 510275, *China*

(Received 2 March 2009; revised manuscript received 21 April 2009)

We theoretically study the beam dynamical behaviour in a modulated optical lattice with a quadratic potential in a photovoltaic photorefractive crystal. We find that two different Bloch oscillation patterns appear for the excitation of both broad and narrow light beams. One kind of optical Landau–Zener tunnelling also appears upon the Bloch oscillation and can be controlled by adjusting the parameter of the optical lattice. Unlike the case of linear potential, the energy radiation due to Landau–Zener tunnelling can be confined in modulated lattices of this kind. For high input intensity levels, the Landau–Zener tunnelling is suppressed by the photovoltaic photorefractive nonlinearity and a symmetry breaking of beam propagation from the modulational instability appears.

Keywords: Bloch oscillation, Landau–Zener tunnelling, double-period lattice, photovoltaic photorefractive
PACC: 4270Q, 7240

1. Introduction

In recent years, light propagation in waveguide arrays and photonic lattices has been the focus of many studies due to its fundamental interest and potential in the novel generation of re-addressable and reconfigurable networks.[1−4] Many intriguing phenomena, such as Bloch oscillation (BO), Landau–Zener tunnelling (LZT) and dynamic localization (DL) in a linear waveguide array or photonic lattice with an external linear optical potential,[5−11] and the discrete (or lattice) solitons and gap solitons in a nonlinear waveguide array or photonic lattice, have been found to be fundamentally different from those observed in homogeneous media.[12−18] In fact, BO and LZT were previously predicted in solid-state physics for electrons in crystalline potentials with an external electrostatic field. However, due to the difficulty in coherent excitation of free electrons, they had not been observed in experiment until 1990s.[19] These fundamental effects exist not only for electron waves but also for electromagnetic waves and matter waves in periodic media under an effective 'electrostatic field' (or 'Coulomb force').[5,6,20−22] In the optical domain, periodic media are built by waveguide arrays or photonic lattices, and the linear optical potential corresponding to a linearly growing effective refractive index can be implemented by adjusting the temperature gradient across a thermo-optic material,[6] by changing the waveguide geometry,[5] by bending the array in the longitudinal direction for waveguide arrays,[23] or by illuminating an incoherent white light with a transversal intensity modulation for photonic lattices in photorefractive crystal.[9] Beautiful optical analogues of BO and LZT have been reported in recent optical experiments.[5,6,8,9] More interesting phenomena have been found in two-dimensional (2-D) photonic lattices, e.g. optical Lissajou-type trajectories, resonant and non-resonant LZT at different symmetry points in a band gap structure of a 2-D hexagonal photonic lattice and a decagonal quasi-periodic photonic lattice.[24−28] In addition, BO and LZT were also observed in BECs in an optical lattice. From the viewpoint of quantum mechanics, the BO and LZT of different coherent waves or quantum particles governed by Schrödinger equations have the same mathematical structures though they have different physical backgrounds. The picture of a quantum harmonic oscillator in a lattice was used to describe BECs and optical phenomena. For BECs, the quadratic potential is produced by focused light fields and sometimes enhanced by magnetic trapping in experiment;[29] for

*Project supported by the National Natural Science Foundation of China (Grant No 10874251).
†Corresponding author. E-mail: shewl@mail.sysu.edu.cn

light propagation in waveguide arrays, the quadratic potential was induced by the rotation of a 1-D waveguide array.[30] In the present paper, we theoretically study the beam dynamical behaviour in a modulated linear or nonlinear optical lattice with a quadratic potential in a photovoltaic photorefractive crystal. We find that the LZT can be controlled by adjusting the parameter of the modulated optical lattice, without the energy of the light beam undergoing BO decay due to the quadratic potential.

2. Theory

Here we consider a signal beam propagating along the z-direction in a bulk photovoltaic photorefractive material. The x-direction is the ferroelectric c axis and the beam is allowed to diffract only along this direction for the (1+1)-D case. The propagation of the signal beam can be described by the following generalized Schrödinger equation in the paraxial approximation and the slowly varying amplitude approximation:

$$\mathrm{i}\,2k_0n_0\frac{\partial E}{\partial z}+\nabla_\perp^2E+2n_0k_0^2n(x,y)E=0, \quad (1)$$

where $n(x,y)$ is the effective modulation of the refractive index, k_0 is the wave number of light in vacuum, and n_0 is the background refractive index of the medium. The function E describes a complex envelope of the optical field of the signal beam. In the following, we will consider the (1+1)-D case , where $\nabla_\perp^2=\partial^2/\partial x^2$.

Considering the photovoltaic effect and neglecting the diffusion effect after Refs.[31] and [32], under the open-circuit condition, we can obtain the expression of $n(x,y)$ based on the band-transport model developed by Kukhtarev *et al*,[33] as follows:

$$\begin{aligned} n(x,y)&=-\frac{1}{2}n_0^3\gamma_{\mathrm{eff}}E_{\mathrm{sc}}\\ &=\frac{1}{2}n_0^3\gamma_{\mathrm{eff}}E_{\mathrm{p}}\frac{S_{\mathrm{s}}I_{\mathrm{s}}+R_{\mathrm{g}}S_{\mathrm{g}}I_{\mathrm{g}}+R_{\mathrm{m}}S_{\mathrm{m}}I_{\mathrm{m}}}{S_{\mathrm{s}}I_{\mathrm{s}}+S_{\mathrm{g}}I_{\mathrm{g}}+S_{\mathrm{m}}I_{\mathrm{m}}+\beta}, \end{aligned} \quad (2)$$

where γ_{eff} is the effective linear electro-optic coefficient; E_{sc} is the space-charge field; E_{p} is the photovoltaic space-charge field; β is the dark generation rate ($I_{\mathrm{d}}=\beta/S_{\mathrm{s}}$ is dark irradiance); S_{s}, S_{g}, S_{m} are the photoionization cross sections corresponding to the signal beam, the modulated lattice beam and the beam that induces a quadratic potential, respectively; R_{g} and R_{m} are the ratios of the Glass coefficients of the lattice beam and the quadratic potential beam respectively to the signal beam respectively. The intensity of the signal beam is $I_{\mathrm{s}}=|E|^2$. Here, we consider such a modulated optical lattice with an intensity profile

$$I_{\mathrm{g}}(x)=I_0\left[\varepsilon\cos^2(\pi x/d_1)+(1-\varepsilon)\cos^2(\pi x/d_2)\right]. \quad (3)$$

Such a modulated lattice potential can be induced by a broad laser beam passing through an appropriately designed amplitude mask or by the interference pattern of two pairs of counterpropagating laser beams. So the lattice spacing and potential well depth are dynamically adjustable, thereby allowing real-time control. In the general case of incommensurate periods d_1 and d_2, the lattice described by expression (3) is quasi-periodic. In the present paper, however, we focus on only the double-period lattice with $d_1=d_2/2$,[34] which is characterized by the parameter ε (which takes values between 0 and 1) and I_0. In addition, we choose such a quadratic potential $I_{\mathrm{m}}(x)=AI_0x^2$ induced by a light beam whose intensity is constant along the crystal length but modulated transversely as shown in Ref.[9]. Clearly, when the crystal is uniformly illuminated by background light, namely, when I_{g} is a constant and $I_{\mathrm{m}}=0$, the expression of E_{sc} reduces into Eq.(6) in Ref.[35] automatically.

Substituting expression (2) into Eq.(1) and adopting the scale transformation $\xi=z/(n_0k_0x_0^2)$, $s=x/x_0$ and $E(s,\xi)=\sqrt{I_0}U(s,\xi)$ (where x_0 is an arbitrary spatial scale), we obtain

$$\mathrm{i}\frac{\partial U(s,\xi)}{\partial\xi}+\frac{1}{2}\frac{\partial^2U(s,\xi)}{\partial s^2}-\alpha V(s)U(s,\xi)=0, \quad (4)$$

where $\alpha=-k_0^2x_0^2n_0^4\gamma_{\mathrm{eff}}E_{\mathrm{p}}/2$,

$$V(s)=\left(|U|^2+R_{\mathrm{g}}S_{\mathrm{g}}I_{\mathrm{g}}/S_{\mathrm{s}}I_0+R_{\mathrm{m}}S_{\mathrm{m}}I_{\mathrm{m}}/S_{\mathrm{s}}I_0\right)\Big/\left(|U|^2+S_{\mathrm{g}}I_{\mathrm{g}}/S_{\mathrm{s}}I_0+S_{\mathrm{m}}I_{\mathrm{m}}/S_{\mathrm{s}}I_0+I_{\mathrm{d}}/I_0\right),$$

and $\alpha V(s)$ is the lattice potential induced by the lattice beam and quadratic potential beam.

3. Simulations

Here we take an iron-doped $LiNbO_3$ photovoltaic photorefractive crystal as the working medium.[32] The wavelengths of the signal beam, lattice beam, and quadratic potential beam are 632.8 nm, 514.5 nm, and 514.5 nm, respectively. Some parameters corresponding to these wavelengths are as follows: n_0 =2.20, $\gamma_{\rm eff} = 30.9$ pV/m, $E_{\rm p} = -27 \times 10^5$ V/m, $R_{\rm g} = R_{\rm m} =$ 2.6, and $S_{\rm s} \approx S_{\rm g} \approx S_{\rm m}$. The typical value of $I_{\rm d}$ is about several mW/cm^2. We set $I_{\rm d}$ at 1 mW/cm^2 as that of I_0. In addition, we set $x_0 = 10$ μm and $d_1 = \pi x_0$.

To understand the dynamical behaviour of the signal beam, we first study the band structure of a linear double-period lattice without quadratic potential. To do this, we ignore the nonlinear term $|U|^2$ in Eq.(4). The band structure of this lattice calculated based on the Bloch theorem is shown in Fig.1. Obviously, there exist several band gaps in the linear spectrum due to their periodicity, and the width of the band gap $E_{\rm g}$ between the first (solid line in Fig.1) and second (dashed line in Fig.1) bands decreases with the increase of ε. We find that the band gap $E_{\rm g}$ plays an important role in the BO and LZT when an external linear optical potential is introduced into this lattice. When $E_{\rm g}$ is large enough, the LZT can be ignored, while when $E_{\rm g}$ is small, the LZT should be taken into account. Therefore, the LZT can be controlled effectively by adjusting the parameter ε. In the following, we will show the influence of ε on the propagation of a light beam in a double-period lattice with a quadratic potential.

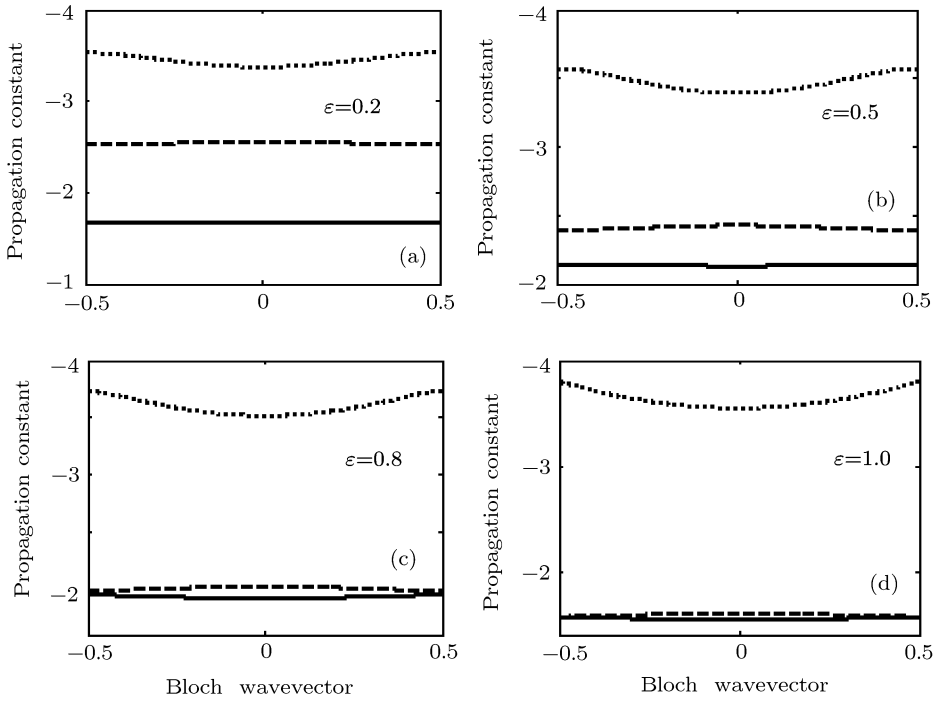


Fig.1. Band structure of a linear double-period lattice for different values of ε, i.e. $\varepsilon = 0.2$ (a); 0.5 (b), 0.8 (c) and 1.0 (d).

Figure 2 shows the profiles of the double-period lattice for different values of ε, where panels (a), (b), (c) and (d) correspond to $\varepsilon = 0.2$, 0.5, 0.8 and 1.0, respectively. Obviously, when ε is close to zero, the period of the lattice potential approaches $d_2 (= 2\pi x_0)$ and the lattice is sparse. However, when ε is close to unity, the period of the lattice potential approaches d_1 and the lattice is dense. In our simulations, $A = 0.01/x_0^2$ is used for the quadratic potential $I_{\rm m}$.

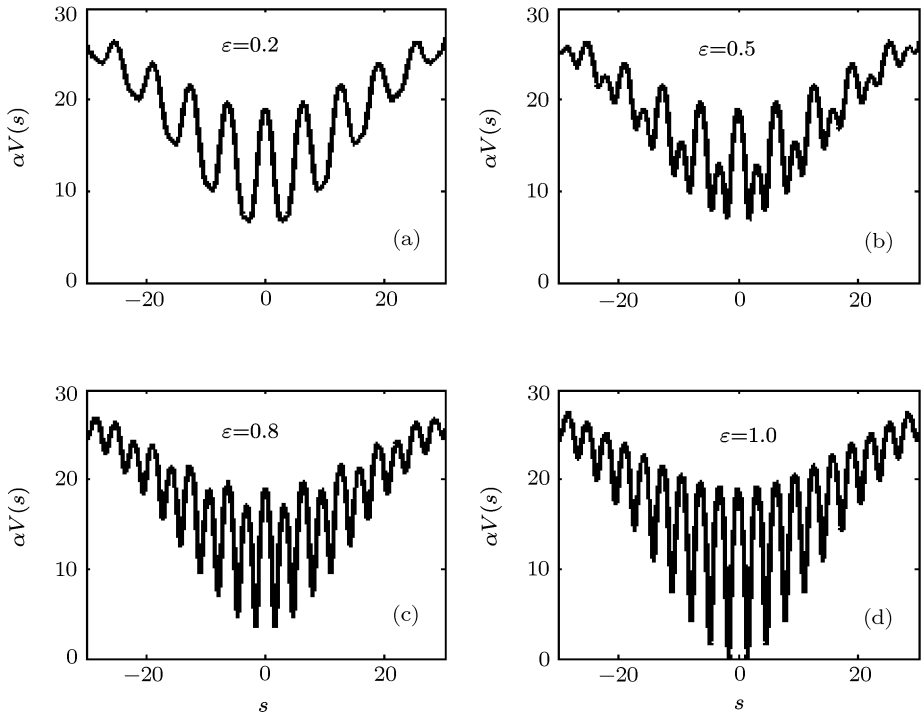


Fig.2. Profiles of a double-period lattice with a quadratic potential for different values of ε, i.e. $\varepsilon = 0.2$ (a), 0.5 (b), 0.8 (c) and 1.0 (d).

3.1. Broad Gaussian beam excitation

We now begin to investigate the dynamical propagation of the signal beam. For simplicity, normal incidence is assumed. An incident Gaussian beam with 100 μm full width at half maximum (FWHM) is used to excite the double-period lattice, shown in Fig.2. The centre of the Gaussian beam is at $s = 0$. We solve numerically Eq.(4) by the standard split-step Fourier method, and the accuracy of the numerical simulation is checked against the total 'power' $\left(\int_{-\infty}^{+\infty} |U|^2 \, \mathrm{d}s\right)$, an invariant of this equation during propagation. The results are shown in Fig.3. For an nW input power level (the central intensity of the incident Gaussian beam is set at 1 μW/cm^2), the beam can hardly feel the nonlinearity. The propagation of the signal beam in this case is shown in the upper part of each picture in Fig.3. For a μW input power level (the central intensity of the incident Gaussian beam is set at 1 mW/cm^2), the nonlinearity of the photorefractive material becomes evident. The propagation of the signal beam is shown in the lower part of each picture in Fig.3.

To understand the behaviour of beam propagation in the double-period lattice shown in Fig.2, we briefly review a Bloch wave (coherent wave in a lattice) or a particle in a linear potential. As is well known, when a Bloch wave or particle in a linear potential reaches the edge of the first Brillouin zone (BZ), the band gap in the frequency domain attains a minimum value and the probability of LZT reaches its maximum value. When LZT happens, the radiation takes place in real space and the energy of the light beam decays,[8] which should consequentially result in the breakdown of BO. Now the linear potential is replaced by a quadratic one for the optical BO, and the energy of the light beam will not decay though the radiation mode still exists, since the radiated energy is confined in the centre of the quadratic potential, as shown in Fig.3. In Fig.3, one sees that the signal beam is scattered into both sides of $s = 0$ by the potential barrier. So the excited Bloch modes locate at the edge of the first BZ. Each scattering branch travels toward the centre of BZ in the frequency domain, where the transverse wave-vector is zero, namely, each scattering branch arrives at the maximum of the transverse position in real space. Then, confined by the quadratic potential, the scattering will come back to the centre of the quadratic potential (corresponding to the edge of BZ), where most of the scattering goes into the radiation mode due to LZT, as shown in Fig.3(a). So, the radiation mode does not result in a loss for the restriction effect of the quadratic potential.

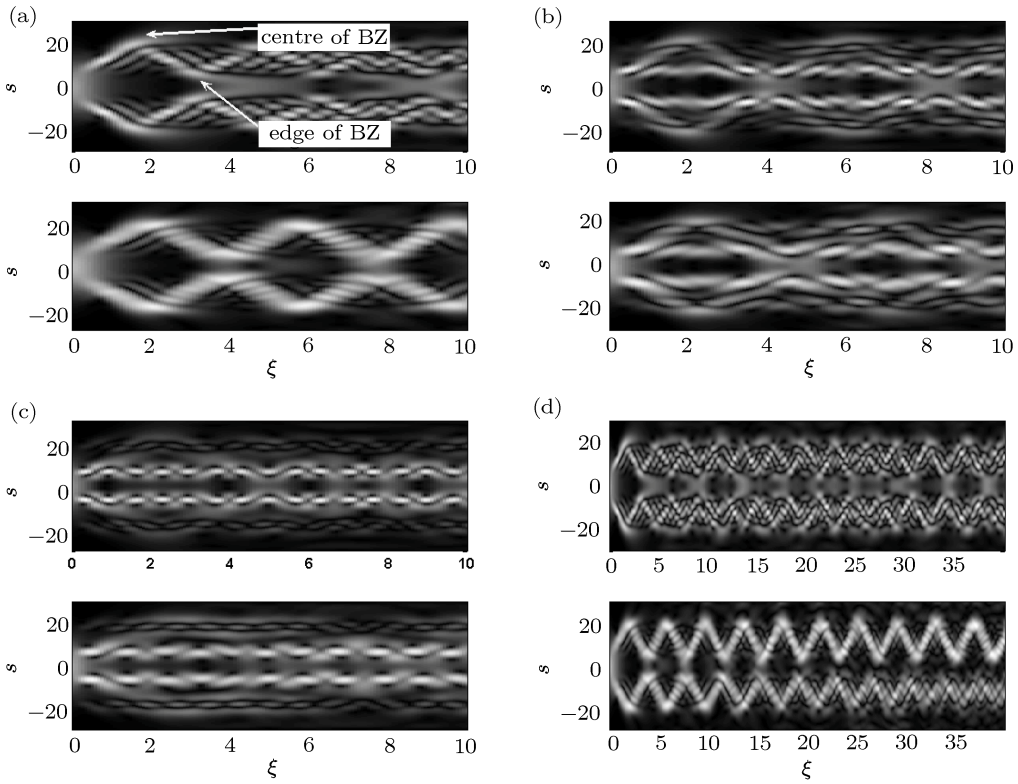


Fig.3. Contours of intensity profile of the propagating beam excited by a broad Gaussian beam at $s = 0$ in a double-period lattice with a quadratic potential for different values of ε, i.e. $\varepsilon = 0.2$ (a), 0.5 (b) and 0.8 (c). The central intensity of the incident beam for the upper part of each picture is 1 μW/cm^2 and for the lower part is 1 mW/cm^2. Panel (d) shows the intensity profile of a beam propagating a long distance, corresponding to the case of panel (a).

It is found that the LZT can be suppressed by the nonlinear effect. For a level of a few mW/cm^2 of input intensity, photorefractive nonlinearity becomes evident and damping of BO becomes slow. This is shown in the lower part of each picture in Fig.3. For a very small value of ε, the LZT is almost suppressed by the photorefractive nonlinearity (as shown in the lower part of Fig.3(a)). Furthermore, an interesting phenomenon of symmetry breaking is observed for 1 mW/cm^2 central intensity and $\varepsilon = 0.2$. Figure 3(d) shows the symmetry breaking clearly. For $\varepsilon = 0.5$ but with the same input power, the symmetry breaking becomes unclear. When the central intensity is further increased to 4 mW/cm^2 and 10 mW/cm^2 for $\varepsilon = 0.5$, it is found that the symmetry breaking appears at 4 mW/cm^2 while it disappears at 10 mW/cm^2 as shown in Fig.4. This symmetry breaking would result from the modulational instability (MI) of the signal beam. The MI is one of the fundamental phenomena existing in many nonlinear systems. In the optics domain, a broad optical beam propagating through a nonlinear medium will undergo MI and develop into a spontaneous pattern or filaments,[36,37] under certain conditions. We now discuss this in detail. Firstly, symmetry breaking appears at 1 mW/cm^2 for $\varepsilon = 0.2$ but not for $\varepsilon = 0.5$. This is because the signal beam is scattered more strongly in the lattice when $\varepsilon = 0.5$ than when $\varepsilon = 0.2$, since the lattice is more complex when $\varepsilon = 0.5$ than when $\varepsilon = 0.2$, as shown in Fig.2. So, the strength of MI in the lattice is weaker when $\varepsilon = 0.5$ than when $\varepsilon = 0.2$. Secondly, when the central intensity is increased to 4 mW/cm^2, the MI is enhanced and the symmetry breaking appears for $\varepsilon = 0.5$. Finally, the symmetry breaking disappears at 10 mW/cm^2. This is not surprising, because it is well known that the photovoltaic photorefractive nonlinearity is saturable and that the MI is suppressed when the nonlinearity of media reaches saturation.[38]

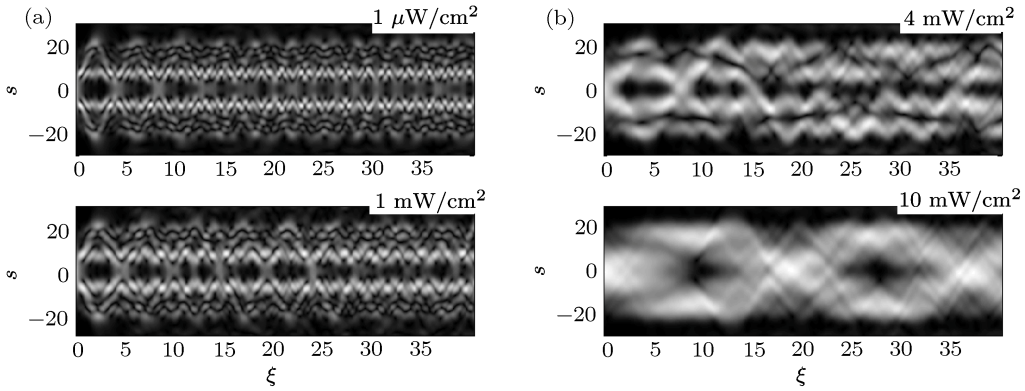


Fig.4. Contours of intensity profile of the propagating beam excited by a broad Gaussian beam at $s = 0$ in a double-period lattice with a quadratic potential, for $\varepsilon = 0.5$. The central intensities of the incident beam in panel (a) are 1 μW/cm^2 and 1 mW/cm^2; and 4 mW/cm^2 and 10 mW/cm^2 in panel (b) for the upper and the lower, respectively.

3.2. Narrow Gaussian beam excitation

In this section, we investigate the dynamical propagation of the signal beam with an initial Gaussian profile of 10 μm FWHM. In this case, the propagation is sensitive to the initial position of the beam. Figures 5 and 6 show the results of the dynamical propagation corresponding to two different centre positions, i.e. $s = 0$ and $-\pi/2$. The upper part and the lower part of each picture in Figs.5 and 6 correspond to the central intensities of the input beam, being 1 μW/cm^2 and 1 mW/cm^2, respectively.

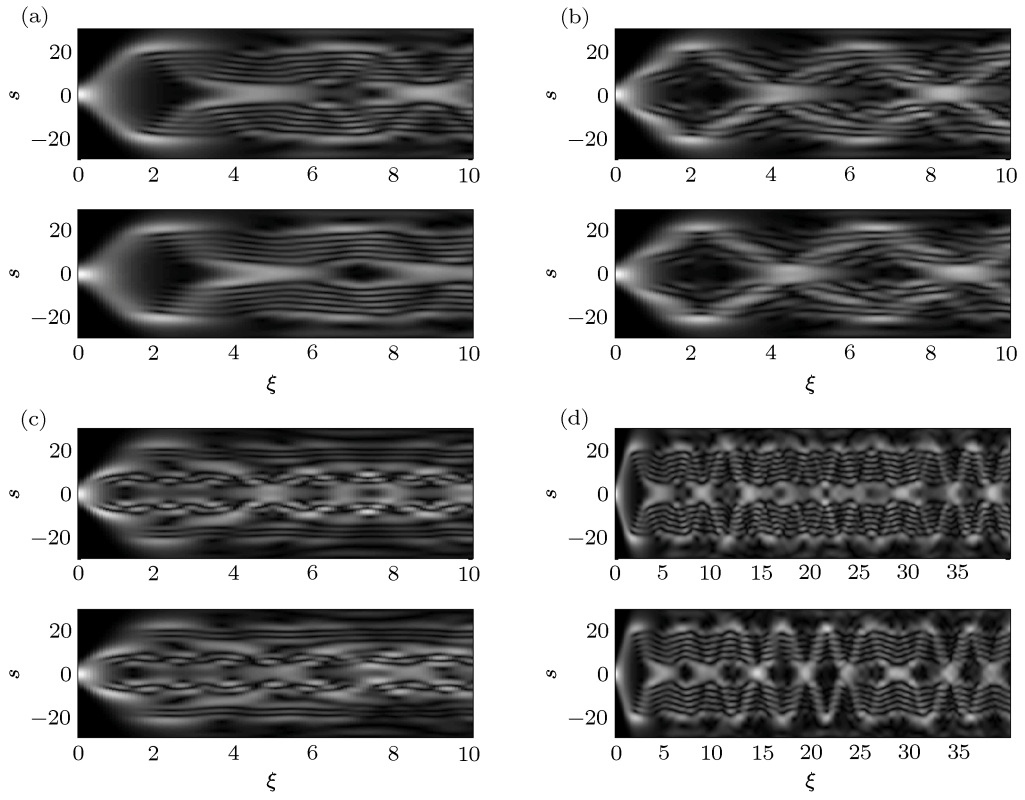


Fig.5. Contours of intensity profile of the propagating beam excited by a narrow Gaussian beam at $s = 0$ in a double-period lattice with a quadratic potential for different values of ε , i.e. $\varepsilon = 0.2$ (a), 0.5 (b), and 0.8 (c). The central intensity of the incident beam for the upper part of each picture is 1 μW/cm^2 and for the lower part is 1 mW/cm^2. Panel (d) shows the intensity profile of a beam propagating a long distance, corresponding to the case of panel (a).

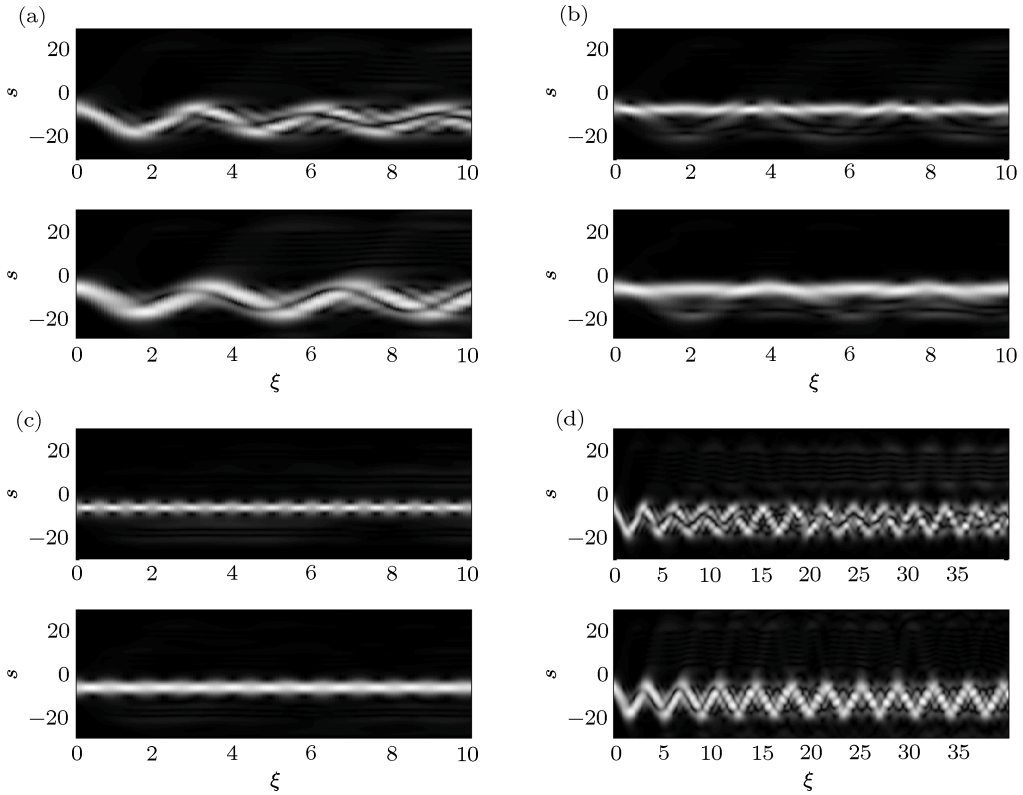


Fig.6. Contour of intensity profile of the propagating beam excited by a narrow Gaussian beam at $s = -\pi/2$ in a double-period lattice with a quadratic potential for different values of ε, i.e. $\varepsilon = 0.2$ (a), 0.5 (b), and 0.8 (c). The central intensity of the incident beam for the upper part of each picture is 1 μW/cm^2 and for the lower part is 1 mW/cm^2. Panel (d) indicates the intensity profile of a beam propagating a long distance, corresponding to the case of panel (a).

For the case of $s = 0$ shown in Fig.5, the signal beam is scattered into both side of the centre by the potential barrier, and then excites most of the modes in the lowest transmission band, which means the excited Bloch modes have a wide space spectrum in BZ. The ripples shown in Fig.5 are due to the BO of these Bloch modes with different wave-vectors. For the broad beam excitation shown in Fig.3(d), the Bloch modes each have a narrow space spectrum, so the trajectory of the beam is narrower than that in Fig.5(d).

For the case of $s = -\pi/2$ shown in Fig.6, the patterns of the signal beam are evidently different from each other, for different values of ε. For $\varepsilon = 0.2$, the signal beam is mostly scattered into one side of $s = -\pi/2$ and a typical damped BO is excited at levels of a few μW/cm^2 and a few mW/cm^2, which is slowed down by the nonlinearity effect, as shown in Fig.6(d). In addition, a little radiation energy caused by LZT is coupled into the other side of $s = -\pi/2$ and confined in this lattice. For $\varepsilon = 0.5$ and 0.8, the scattering becomes weak because of a potential well at $s = -\pi/2$ (shown in Figs.2(b) and 2(c)). In this case, the transverse momentum of the beam is too small to cross over the potential barriers of both sides and can only propagate in the potential well, as shown Figs.6(b) and 6(c). It should be noted that, at a few μW input power level, a quasi-soliton (bright soliton) can be excited for $\varepsilon = 0.8$, which is shown in the lower part of Fig.6(c). For the defocusing photorefractive nonlinearity of a $LiNbO_3$ crystal, the bright soliton can be excited under a background laser beam or an optically induced periodic lattice.[32,39] So we believe that the bright soliton can exist in a double-period lattice with a quadratic potential.

4. Conclusion

We theoretically investigate the beam dynamical behaviour in a photovoltaic photorefractive crystal, in which there is a modulated linear or nonlinear optical lattice with a quadratic potential. Damped BO accompanied by LZT results in different beam patterns for both broad and narrow beam excitations. The beam

patterns can be controlled by adjusting the parameter of the lattice. Unlike the linear potential, the energy radiation caused by LZT can be confined in this kind of lattice. In addition, for high input power levels, the photorefractive nonlinearity causes symmetry breaking and the suppression of LZT.

References

[1] Eisenberg H S, Silberberg Y, Morandotti R, Boyd A R and Aitchison J S 1998 *Phys. Rev. Lett.* **81** 3383

[2] Morandotti R, Peschel U, Aitchison J S, Eisenberg H S and Silberberg Y 1999 *Phys. Rev. Lett.* **83** 2726

[3] Christodoulides D N, Lederer F and Silberberg Y 2003 *Nature* **424** 817

[4] Fleischer J W, Segev M, Efremidis N K and Christodoulides D N 2003 *Nature* **422** 147

[5] Morandotti R, Peschel U, Aitchison J S, Eisenberg H S and Silberberg Y 1999 *Phys. Rev. Lett.* **83** 4756

[6] Pertsch T, Dannberg P, Elflein W, Brauer A and Lederer F 1999 *Phys. Rev. Lett.* **83** 4752

[7] Fratalocchi A, Assanto G, Brzdakiewicz K A and Karpierz M A 2006 *Opt. Lett.* **31** 790

[8] Trompeter H, Pertsch T, Lederer F, Michaelis D, Streppel U, Bräuer A and Peschel U 2006 *Phys. Rev. Lett.* **96** 023901

[9] Trompeter H, Krolikowski W, Neshev D N, Desyatnikov A S, Sukhorukov A A, Kivshar Y S, Pertsch T, Peschel U and Lederer F 2006 *Phys. Rev. Lett.* **96** 053903

[10] Lenza G, Parkerb R, Wankea M C and de Sterke C M 2003 *Opt. Commun.* **218** 87

[11] Longhi S, Marangoni M, Lobino M, Ramponi R, Laporta P, Cianci E and Foglietti V 2006 *Phys. Rev. Lett.* **96** 243901

[12] Mandelik D, Eisenberg H S, Silberberg Y, Morandotti R andAitchison J S 2003 *Phys. Rev. Lett.* **90** 053902

[13] Martin H, Eugenieva E D, Chen Z and Christodoulides D N 2004 *Phys. Rev. Lett.* **92** 123902

[14] Neshev D N, Alexander T J, Ostrovskaya E A, Kivshar Y S, Martin H, Makasyuk I and Chen Z 2004 *Phys. Rev. Lett.* **92** 123903

[15] Fleischer J W, Bartal G, Cohen O, Manela O, Segev M, Hudock J and Christodoulides D N 2004 *Phys. Rev. Lett.* **92** 123904

[16] Yang J, Makasyuk I, Bezryadina A and Chen Z 2004 *Stud. App. Math.* **113** 389

[17] Yang J, Makasyuk I, Kevrekidis P G, Martin H, Malomed B A, Frantzeskakis D J and Chen Z 2005 *Phys. Rev. Lett.* **94** 113902

[18] Chen F, Stepić M, Rüter C, Runde D, Kip D, Shandarov V, Manela O and Segev M 2005 *Opt. Express* **13** 4314

[19] Waschke C, Roskos H G, Schwedler R, Leo K, Kurz H and Kohler K 1993 *Phys. Rev. Lett.* **70** 3319

[20] Morsch O, Müller J H, Cristiani M, Ciampini D and Arimondo E 2001 *Phys. Rev. Lett.* **87** 140402

[21] Konotop V V, Kevrekidis P G and Salerno M 2005 *Phys. Rev. A* **72** 023611

[22] Salerno M, Konotop V V and Bludov Y V 2008 *Phys. Rev. Lett.* **101** 030405

[23] Lenz G, Talanina I and de Sterke C M 1999 *Phys. Rev. Lett.* **83** 963

[24] Witthaut D, Keck F, Korsch H J and Mossmann S 2004 *New J. Phys.* **6** 41

[25] Shchesnovich V S, Cavalcanti S B, Hickmann J M and Kivshar Y S 2002 *Phys. Rev.* E **74** 056602

[26] Desyatnikov A S, Kivshar Y S, Shchesnovich V S, Cavalcanti S B and Hickmann J M 2007 *Opt. Lett.* **32** 325

[27] Shchesnovich V S 2007 *Phys. Rev.* B **76** 115130

[28] Brazhnyi V A, Konotop V V, Kuzmiak V and Shchesnovich V S 2007 *Phys. Rev.* A **76** 023608

[29] Blakie P B and Wang W X 2007 *Phys. Rev.* A **76** 053620

[30] Longhi S 2007 *Phys. Rev.* B **76** 195119

[31] Segev M, Valley G C, Bashaw M C, Taya M and Fejer M M 1997 *J. Opt. Soc. Am.* B **14** 1772

[32] She W L, Xu C C, Guo B and Lee W K 2006 *J. Opt. Soc. Am.* B **23** 2121

[33] Kukhtarev N V, Markov V B, Odulov S G, Soskin M S and Vinetskii V L 1979 *Ferroelectrics* **22** 949

[34] Louis P J Y, Ostrovskaya E A and Kivshar Y S 2005 *Phys. Rev.* A **71** 023612

[35] Anastassiou C, Shih M, Mitchell M, Chen Z and Segev M 1998 *Opt. Lett.* **23** 924

[36] Arecchi F T, Boccaletti S and Ramazza P 1999 *Phys. Rep.* **318** 1

[37] Zhang B Z, Cui H and She W L 2009 *Chin. Phys.* B **18** 209

[38] Kip D, Soljačić M, Segev M, Eugenieva E and Christodoulides D N 2000 *Science* **290** 495

[39] Zhang B Z, Wang H C, Cui H and She W L 2008 *J. Opt.* A: *Pure Appl. Opt.* **10** 015101